

Electrically switchable finite energy Airy beams generated by a liquid crystal cell with patterned electrode

D. Luo, H.T. Dai, X.W. Sun*, H.V. Demir

School of Electrical and Electronic Engineering, Nanyang Technological University, Nanyang Avenue, Singapore 639798, Singapore

ARTICLE INFO

Article history:

Received 17 February 2010

Received in revised form 21 May 2010

Accepted 26 May 2010

Keywords:

Diffraction

Liquid crystal devices

Propagation

ABSTRACT

A pair of electrically switchable finite energy Airy beams is generated by a liquid crystal (LC) cell, where one electrode is patterned by a photomask with a binary-phase pattern. Applying voltage across the LC cell, an index modulation is produced due to the liquid crystal molecules realignment, and the finite energy Airy beams can be generated or erased corresponding to the phase difference between the regions with and without electrode. The diffraction-free and transverse acceleration dynamics of this binary-phase element based finite energy Airy beams were experimentally verified, exhibiting excellent agreement with the theory.

© 2010 Elsevier B.V. All rights reserved.

1. Introduction

Accelerating finite energy Airy beams is a kind of diffraction-free beams with intriguing free acceleration during propagation [1,2]. The Airy beam is related to the non-spreading Airy wave packets firstly studied by Berry and Balazs within the context of quantum mechanics [3]. Recently, there is a surge of studies of finite energy Airy beam [4–9], with potential applications in optical manipulation [10,11] and plasma channel generation [12].

Several methods including spatial light modulator (SLM) [2], continuous phase mask [12], and even nonlinear photonic crystal were reported to generate Airy beams previously [11]. However, all of these methods mentioned above possessed either high cost or complicated fabrication process. In contrast, optical elements with binary-phase pattern could be fabricated easily with lower cost, which provides a simple way to generate optical beams such as Airy beams. Therefore, it is useful and meaningful to study the properties of Airy beams produced by such optical binary-phase elements.

On the other hand, liquid crystal (LC) has tunable refractive properties, and it has been applied in realizing tunable diffractive optical elements (e. g., Fresnel zone plate [13–16], optical vortex [17,18], etc.). We have recently demonstrated polymer-dispersed liquid crystal (PDLC) based binary-phase pattern to generate Airy beam [19], however, the phase modulation is only about 0.3π , and a larger phase modulation cannot be achieved using PDLC. In this paper, we demonstrate electrically switchable finite energy Airy beams generated by a liquid crystal cell with binary-phase patterned

electrode. Both of the electrical tunable properties and the propagation characteristics of the Airy beams are investigated in detail.

The finite energy Airy beams can be realized by adding an exponential aperture function on the Airy function in the initial condition, i.e., $\phi(s, \xi=0) = Ai(s)\exp(as)$ [1], where ϕ is the electric field envelope, $s = x/x_0$ represents a dimensionless transverse coordinate, x_0 is an arbitrary transverse scale, $\xi = z/kx_0^2$ is used to normalize the propagation distance z , $k = 2\pi n/\lambda_0$ is the wavenumber of the optical wave with the index of refraction n and wavelength λ_0 in vacuum, and a is a positive parameter. For $a \ll 1$, the resulting finite energy Airy beams closely resembles the Airy functions. The finite energy Airy beam can be expressed as [2]:

$$\phi(\xi, s) = Ai\left[s - (\xi/2)^2 + ia\xi\right] \times \exp\left[as - (a\xi^2/2) - i(\xi^3/12) + i(a^2\xi/2) + i(s\xi/2)\right] \quad (1)$$

The Fourier transform $\Phi_0(k)$ of this truncated Airy wave packet, which is proportional to $\Phi_0(k) \propto \exp(-ak^2)\exp(ik^3/3)$ [2], can be treated as a Gaussian function modulated by a cubic phase. Here, a broad Gaussian beam with a cubic phase imposed on it can be used to generate the finite energy Airy beam optically.

2. Experiment

In 2D case, the initial field envelope of finite energy Airy wave packets can be given by: $\phi(s_x, s_y, \xi=0) = Ai(s_x)Ai(s_y)\exp[a(s_x + s_y)]$, where $s_x = x/x_0$, $s_y = y/y_0$. The Fourier transform can be written as: $\Phi_0(k_x, k_y) \propto \exp[-a(k_x^2 + k_y^2)] \exp[i(k_x^3 + k_y^3)/3]$, where k_x and k_y are Fourier spectrum coordinates.

* Corresponding author. Tel.: +65 67905369.

E-mail address: exwsun@ntu.edu.sg (X.W. Sun).

Fig. 1(a) shows a 2D continuous phase pattern of an Airy wave packet. The phase range of this pattern varies from -11.5π to $+11.5\pi$ in 0.43 cm , which has been wrapped between 0 and 2π . In our experiment, the binary-phase pattern with cubic phase modulation was obtained by converting the continuous phase pattern by setting the value of phase delay between $0\sim\pi$ as 0 and $\pi\sim 2\pi$ as π , respectively. This binary-phase pattern is shown in Fig. 1(b), where the black and white regions represent phase values of 0 and π , respectively. Then, the binary-phase pattern was transferred to a transparent mask, using a patterned indium–tin-oxide (ITO)-coated glass substrate that was obtained by a standard photolithography process.

The patterned ITO glass was then used to assemble a LC cell with a blank ITO glass as the counter electrode. The LC cell was prepared by anti-parallel rubbing. The cell gap was $d=7.5\ \mu\text{m}$ controlled by spacers. The liquid crystal used in our experiment was E7 from Merck, with $n_o = 1.5216$ and $n_e = 1.7462$.

When the voltage is applied across the LC cell, LC molecules in the region with ITO electrode will reorient according to the external voltage, while the LC molecules in the region without ITO electrode will remain unchanged. Fig. 1(c) and (d) show the optical microscopic images of the LC cell sandwiched between two cross polarizers at applied voltage levels of $3V_{\text{rms}}$ and $9V_{\text{rms}}$, respectively. The rubbing direction of LC cell was at 45° with respect to both polarizer and analyzer axes. As the voltage exceeds the threshold ($\sim 0.81V_{\text{rms}}$), the LC directors in the regions with ITO electrode start to reorient, as reflected by the color change as shown in Fig. 1(c). In the high voltage regime ($\sim 9V_{\text{rms}}$), the LC directors in the regions with ITO electrode are reoriented nearly perpendicular to the substrates, leading to a black state as shown in Fig. 1(d).

If the polarization of the incident light is parallel to the rubbing direction of the cell, the phase difference ($\Delta\delta$) between the regions with and without ITO electrode under the external voltage can be expressed as $\Delta\delta = \frac{2\pi}{\lambda}(n_e - n_{\text{eff}}) \cdot d$, where d is the cell gap, λ is the wavelength of incident light, and n_{eff} is effective LC refractive index in the region with ITO electrode.

The LC cell sample recorded with binary cubic phase pattern was illuminated by a collimated He–Ne laser (633 nm) with a beam diameter of about 1 cm to generate the finite energy Airy beams. A

polarizer was used to ensure the polarization of incident light was parallel to the rubbing direction of LC cell sample. A spherical lens ($f=20\text{ cm}$) placed at a distance of f behind the LC cell sample was used to perform the Fourier transform of the binary-phase pattern. The Fourier transform or finite energy Airy beam was obtained at a distance of $d=f$ behind the lens, and then captured by a charge-coupled-device (CCD) camera. The optical setup is illustrated in Fig. 1(e).

3. Results and discussions

The initial phase difference between the regions with and without ITO electrode is zero. The Airy beams would be generated (e.g. at voltages of $1.08V_{\text{rms}}$, $1.69V_{\text{rms}}$ and $6.0V_{\text{rms}}$) when the phase difference is the odd integer times of π , and the Airy beams would be erased (e.g., at voltages of $1.31V_{\text{rms}}$ and $2.29V_{\text{rms}}$) when the phase difference is the even integer times of π . Fig. 2(a), (b), and (c) show the observed intensity distribution of 2D Airy wave packet under voltages of $1.08V_{\text{rms}}$, $1.25V_{\text{rms}}$ and $1.31V_{\text{rms}}$, at $z=9.0\text{ cm}$, respectively. The coordinate system is also labeled in Fig. 2(a). We can see that the 2D finite energy Airy beams were generated in Fig. 2(a), blurred in Fig. 2(b), and erased in Fig. 2(c). In Fig. 2(c), we can see that the Airy beam is not completely erased as some strong diffraction spots exist, which is primarily caused by the fringe field at the edge of the patterned electrode. With voltage applied on the patterned electrode, the electric field lines will bend into those regions uncovered by the electrode especially at the electrode edge. Thus some liquid crystals in the regions without electrode will be slightly influenced by the electric field. This “error” state of liquid crystals will lead to an error phase at the electrode edge, i.e. there is no perfect phase contrast between the regions with and without electrode, and hence an uncompleted erased image appears. It is worth mentioning that the generated image consisted of a pair of symmetric Airy beams with opposite propagation directions, which was due to the intrinsic property of binary element. When the applied voltage was larger than $6.0V_{\text{rms}}$, the generated image did not show significant change, indicating the LC directors in the region with ITO electrode were reoriented almost along the electric field and the phase difference would not change anymore.

To better understand the 2D finite energy Airy beams from binary-phase element, several simulated images on x - y plane, calculated using Angular Spectrum Method from GWO library [20,21], are shown

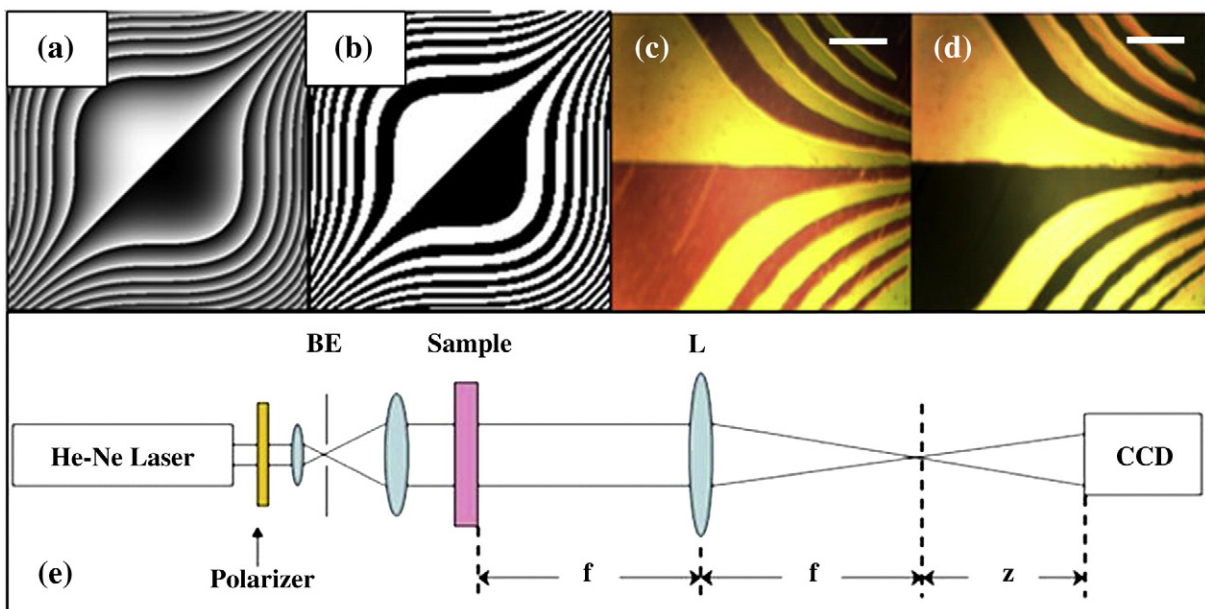


Fig. 1. (a) Continuous phase mask and (b) the corresponding binary-phase mask used to generate the 2D Airy beam. Optical microscopic images of the LC cell sandwiched between two cross polarizers at applied voltage of (c) $3V_{\text{rms}}$ and (d) $9V_{\text{rms}}$. The scale bar in (c) and (d): 0.5 cm . (e) Optical setup for Airy beam reconstruction (BE, beam expander and L, lens).

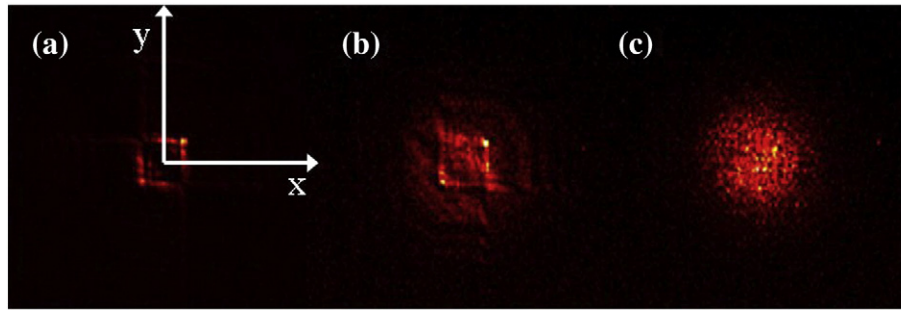


Fig. 2. The observed intensity distribution of the 2D Airy wave packets under different levels of external applied voltages of (a) $1.08V_{\text{rms}}$, (b) $1.25V_{\text{rms}}$, and (c) $1.31V_{\text{rms}}$, at $z = 9.0$ cm.

in Fig. 3(a)–(d) at different distances of $z = 4.0$ cm, 7.0 cm, 8.5 cm, and 10.0 cm, respectively. The simulation was used to describe the propagation of the Airy beam generated by the binary-phase pattern, its parameters were set according to the real experimental setup with binary-phase pattern sample size of $0.43 \text{ cm} \times 0.43 \text{ cm}$, a Fourier transform lens ($f = 20$ cm), and π phase difference between the regions with and without ITO electrode. The corresponding images obtained from experiment at applied voltage of $1.08V_{\text{rms}}$ (where $\Delta\delta = \pi$ is obtained) are also shown in Fig. 3(e)–(h), respectively, which are consistent with the simulated images. Because of the twin lobes of Airy beams generated from binary element, the two Airy beams maximum intensity points were overlapped (Fig. 3(e)) before $z = 6.5$ cm. After that distance, these twin Airy beams then separated with each other and propagated along the bisection direction of x - and y -axis with opposite directions (Fig. 3(f)–(h)). This overlap property of the twin Airy beams arisen from the binary-phase element is not possessed by the Airy beam produced using spatial light modulator (SLM) with continuous phase modulation. To obtain the detail transverse profile of the Airy beam, an objective lens was located just before the CCD camera for magnification purpose. Fig. 4 shows the magnified transverse profile of the 2D finite energy Airy beam from

the applied voltage of $1.08V_{\text{rms}}$, at $z = 10.5$ cm. Only one group of Airy beam was captured here.

In order to study the propagation dynamics of the 2D finite energy Airy wave packet, we further investigated the relationship between the deflection along the bisector direction of x - and y -axis and propagation distance (Fig. 5), where the voltage applied across the LC cell was fixed at $1.08V_{\text{rms}}$. In Fig. 5, the red triangles represent the simulated results based on beam propagation simulation. The blue circles represent the experimental results and the green line is a parabolic fit. We can see that the relationship of the deflection and propagation distance is parabolic, and the experimental results are quite consistent with the simulation. The parabolic relationship indicates that the Airy beams produced from the binary-phase element possess a transverse acceleration, which is the same as Airy beams generated from continuous phase modulation. In our experiment, the Airy beams moved on a 2D parabolic trajectory with $x_d = y_d$, where x_d and y_d were the transverse deflections in x and y directions respectively. This parabolic trajectory is a result of acceleration and can be well described by $x_d \cong \lambda_0^2 z^2 / (16\pi^2 x_0^3)$ (the parabolic fit presented in Fig. 5) [2]. The deflection in Fig. 5, which represents the parameter of $\sqrt{2}x_d$, shows a shift of $459.5 \mu\text{m}$ within

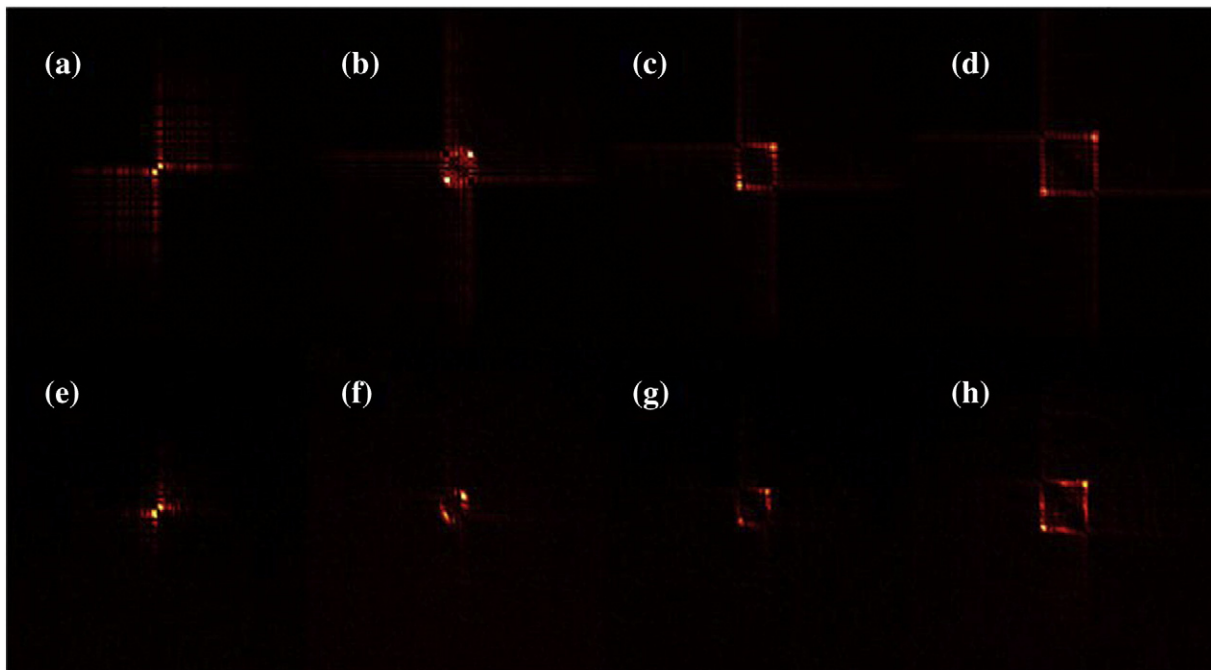


Fig. 3. Simulated images of Airy beams in x - y plane at a distance of (a) $z = 4.0$ cm, (b) 7.0 cm, (c) 8.5 cm, and (d) 10.0 cm, setting phase difference of π ; corresponding experimental images at the same distances of (e) $z = 4.0$ cm, (f) 7.0 cm, (g) 8.5 cm, and (h) 10.0 cm, at applied voltage of $1.08V_{\text{rms}}$.

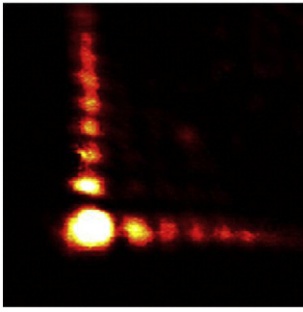


Fig. 4. Two dimensional finite energy Airy beam captured by a CCD with an additional objective lens for the applied voltage of $1.08V_{rms}$, at $z = 10.5$ cm.

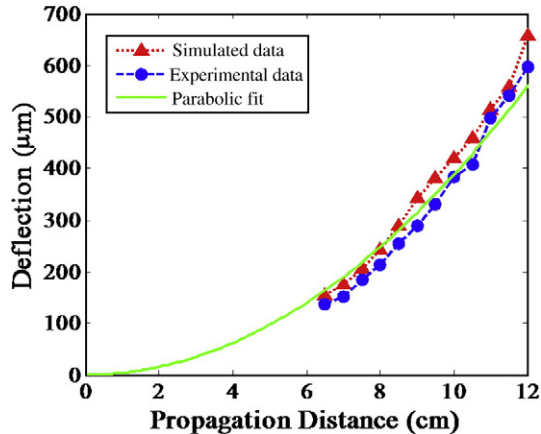


Fig. 5. Acceleration of the 2D Airy beam along the bisector direction of x - and y -axis as a function of distance. The red triangles represent the simulated results, the blue circles represent the experimental results, and the green line shows the parabolic fit curve.

5.5 cm propagation distance. The value of $x_0 = 45.2 \mu\text{m}$ was calculated here and the Airy beams propagated almost diffraction-free up to a distance of ~ 12 cm. This relatively small propagation distance is due to the small focal length of lens and the big size of LC sample.

4. Conclusion

In conclusion, a pair of electrically switchable 2D finite energy Airy beams has been generated by a liquid crystal cell with binary-phase patterned electrode. These Airy beams are electrically switchable, which can be generated or erased with the change of applied electric field. The diffraction-free and transverse acceleration dynamics of the Airy beams were verified. This kind of binary-phase element based Airy beam device has the advantages of low cost, easy fabrication process, and electrical tunability, potentially useful in adaptive optics.

Acknowledgements

This work was partially supported by a Poland–Singapore collaborative project sponsored by Agency for Science, Technology and Research of Singapore (no. 062 120 0016). The authors are grateful to Tomoyoshi Shimobaba for providing the GWO library, <http://sourceforge.net/projects/thegwolibrary/>.

References

- [1] G.A. Siviloglou, D.N. Christodoulides, *Opt. Lett.* 32 (2007) 979.
- [2] G.A. Siviloglou, J. Broky, A. Dogariu, D.N. Christodoulides, *Phys. Rev. Lett.* 99 (2007) 213901.
- [3] M.V. Berry, N.L. Balazs, *Am. J. Phys.* 47 (1979) 264.
- [4] I.M. Besieris, A.M. Shaarawi, *Opt. Lett.* 32 (2007) 2447.
- [5] M.A. Bandres, J.C. Gutiérrez-Vega, *Opt. Express* 15 (2007) 16719.
- [6] G.A. Siviloglou, J. Broky, A. Dogariu, D.N. Christodoulides, *Opt. Lett.* 33 (2008) 207.
- [7] H.I. Sztul, R.R. Alfano, *Opt. Express* 16 (2008) 9411.
- [8] P. Saari, *Opt. Express* 16 (2008) 10303.
- [9] J. Broky, G.A. Siviloglou, A. Dogariu, D.N. Christodoulides, *Opt. Express* 16 (2008) 12880.
- [10] J. Baumgartl, M. Mazilu, K. Dholakia, *Nat. Photonics* 2 (2008) 675.
- [11] T. Ellenbogen, N.V. Bloch, A.G. Padowicz, A. Arie, *Nat. Photonics* 3 (2009) 395.
- [12] P. Polynkin, M. Kolesik, J.V. Moloney, G.A. Siviloglou, D.N. Christodoulides, *Science* 324 (2009) 229.
- [13] Y.-H. Fan, H.W. Ren, S.-T. Wu, *Opt. Express* 13 (2005) 4141.
- [14] L.-C. Lin, H.-C. Jau, T.-H. Lin, A.Y.-G. Fuh, *Opt. Express* 15 (2007) 2900.
- [15] K.-T. Cheng, C.-K. Liu, C.-L. Ting, A.Y.-G. Fuh, *Opt. Express* 17 (2007) 14078.
- [16] K.-C. Lo, J.-D. Wang, C.-R. Lee, T.-S. Mo, *Appl. Phys. Lett.* 91 (2007) 181104.
- [17] Y.J. Liu, X.W. Sun, Q. Wang, D. Luo, *Opt. Express* 15 (2007) 16645.
- [18] Y.J. Liu, X.W. Sun, D. Luo, Z. Raszewski, *Appl. Phys. Lett.* 92 (2008) 101114.
- [19] H.T. Dai, X.W. Sun, D. Luo, Y.J. Liu, *Opt. Express* 17 (2009) 19365.
- [20] T. Shimobaba, Y. Sato, J. Miura, M. Takenouchi, T. Ito, *Opt. Express* 16 (2008) 11776.
- [21] T. Shimobaba, T. Ito, N. Masuda, Y. Abe, Y. Ichihashi, H. Nakayama, N. Takada, A. Shiraki, T. Sugie, *J. Opt. A: Pure Appl. Opt.* 10 (2008) 075308.